Supplementary Text

Patient 5

At the NIH Clinical center there were a total of 5 patients with MDRAB in whom colistin resistance evolved. The four patients discussed in the main text were taken off colistin and demonstrated a loss of colistin resistance. The fifth patient was never removed from colistin, thereby not allowing us to follow the fate of their resistance mutations. However, we sequenced and analyzed patient 5's isolates to understand the mechanism of resistance, and the functional implications of this. As with the other four patients, colistin resistance in patient 5 was associated with a mutation to *pmrB*, and increased expression of the *pmr* locus (Figure S5).

In vitro growth rates of patient isolates

Previous work has demonstrated an *in vitro* fitness cost associated with colistin resistance in *A. baumannii*(López-Rojas et al. 2011; Fernández-Reyes et al. 2009; Rolain et al. 2011). To verify that this was the case with resistant isolates from the five patients in this study we measured *in vitro* growth curves for each set of patient isolates. While there is generally a growth defect associated with resistance (Figure S2), there are nuances specific to each patient, which we believe are a product of each lineages unique evolutionary trajectory.

PT1

In PT1 there is a statistically significant growth defect in the resistant mutant (PT1-S vs. PT1-R, t-test $p = 0.002$). Interestingly, this defect is not completely restored in the post-colistin susceptible isolate (PT1-S vs. PT1-S', t-test $p = 0.02$), despite return of the *pmr* transcript to baseline levels. We therefore hypothesized that the decreased growth of PT1-S' is a consequence of one of the non-*pmr* mutations in PT1-S' relative to PT1-S. We hypothesized that the most likely candidate is the mutation to EF-Tu, which plays a central role in protein translation. Interestingly, we observed mutations to the translational machinery in several resistant mutants. We hypothesized that the recurrent nature of these mutations indicates that they might be compensating for the decreased growth of resistant mutants. It has

previously been shown that decreasing the translation rate can prove beneficial in mutants with compromised growth capacities, by preventing wasteful translation[Bollenbach et al. 2009]. If this is the case, then once the growth cost associated with elevated *pmr* activity is alleviated in PT1-S', the potential growth rate is restored to wild-type, and the mutation to the translational machinery is now growth limiting.

PT2

In PT2 there is again a growth defect associated with resistance (PT2-S vs. PT2-R, t-test p = 0.04). This defect is completely restored in the post-colistin susceptible isolate (PT2-S'). Of note, PT2 also has a mutation to the translational machinery, specifically to an aspartyl tRNA synthetase. However, despite the fact that this mutation remains in PT2-S', there is no associated fitness cost. It is possible that we cannot detect the growth defect in our growth assay, or that the mutation is in fact not deleterious. It is of note that we predict that the amino acid change in the aspartyl tRNA synthetase to be deleterious based on SIFT, which looks at the evolutionary conservation at a given position across the protein family.

PT3

In PT3 there is not a significant difference in the growth rate of susceptible and resistant isolates. The disappearance of the resistant strain from this patient upon termination of colistin treatment indicates that there is in fact an *in vivo* fitness-cost. It is possible that the fitness cost of this mutation is not detected *in vitro*, although this would be somewhat surprising given the ability to detect fitness defects associated with similar mutations in the other mutations. Another possibility is that our numerical representation of the growth curve by a single growth rate misses more nuanced growth defects. Evidence for this is an observed longer lag-phase in the resistant mutant from this patient (data not shown).

PT4

PT4 is of special interest, as we predict that the initial isolate, PT4-S, is already colistin resistant. Strikingly, the isolates for this patient do not show the same trend of a decreased growth rate associated with increasing MIC. This may be because the initial isolate may have already paid the fitness cost, and additional mutations do not have an effect. Alternatively, one or several of the additional mutations relative to PT2-S (Figure S3, see below) may have helped to compensate for the *pmr* associated fitness defect.

PT5

PT5's isolates largely follow the trend of decreased growth rate with increased MIC. The exception is the last isolate (PT5-Re), which fails to recover the fitness cost of earlier resistant isolates, despite having a lower MIC. It is hard to assess the significance of this, as this is the final isolate for this patient, and it is unknown if it would have been a stable genotype. However, a strong candidate for enacting a fitness cost is the *rpoB* mutation unique to PT5-Re. This mutation is predicted to be deleterious based on SIFT.

Identification of putative transmitters and recipients of PT4's strain

The finding that PT4's initial strain appeared to be colistin resistant raised two questions: 1) In whom had this strain evolved colistin resistance? and 2) Had this strain been transmitted to any additional patients? To address this we sequenced the *pmr* locus in patient isolates that were the same strain type as PT4 (pulsotype B, Figure S1), and were isolated in the year before or after PT4's first isolate. For patients before PT4, we sequenced several isolates to attempt to observe the evolution of resistance. For patients after PT4 we sequenced only the initial isolate, to determine if PT4's isolate had been transmitted. There were a total of four patients with *A. baumannii* strains of type B isolated in the year before or after PT4. Two of these were before PT4 (PTA and PTB, Figure S4) and two were after (PTC and PTD, Figure S4). Of the two after, PTD had the same pmr genotype as PT4, and also overlapped with PT4 in the ICU, suggesting a possible transmission from PT4 to PTD. Of the two before, PTA had no *pmr* mutations, but PTB showed evidence of

being the origin of PT4's genotype. PTB's initial isolate had no *pmr* mutations, but later isolates, after receiving colistin, show the same mutation present in the *pmr* of PT4-S. Furthermore, PTB also overlapped with PT4 in the ICU during a time frame that could account for a transmission from PTB to PT4. Thus, we hypothesize that this putative stably colistin resistant isolate evolved undetected in PTB, and was subsequently transmitted to PT4 and PTD.

Genomic variation between initial isolates of PT2 and PT4

To gain insight into the genetic basis for colistin resistance in the initial isolate of PT4, it was compared to the initial isolate of PT2, as both are of strain type B (See Figure S1). It was found that the two differed by a total of 8 non-synonymous mutations (Figure S4), excluding those present in recombinant regions (See below). Of these 8, one was in *pmrB*, which we hypothesize resulted in increased expression of the *pmr* transcript (main text Figure 4) and colistin resistance (Table S4). Also of note among the 8 mutations was another mutation in the translational machinery, specifically to a lysyl tRNA synthestase. This again fits with the hypothesis that translational mutations help compensate for the fitness cost of *pmr* mutations.

In addition to single nucleotide variants, there are some large indels distinguishing the PT2-S and PT4-S. In particular, PT4-S has acquired region containing genes believed to play a role in iron acquisition(Antunes et al. 2010). In previous work we demonstrated that this region, along with three others, were frequently switched out in *A. baumannii* via a homologous recombination (Snitkin et al. 2011). The genome of PTS-4 shows an increased density of variants relative to PTS-2 surrounding this acquired region, supporting the role of recombination. Thus, bolstering the relevance of our previous findings, we observe a recombination mediated acquisition event that occurred in a patient during the course of an outbreak, as PT2-S occurred early in the outbreak and PT4-S more than one year later. Future work is required to better understand the tradeoffs involved in gaining and losing this iron acquisition locus. A simple hypothesis is a tradeoff between the benefit of

more efficiently acquiring iron from a host, vs. the detrimental effect of having this region if it becomes a target of an adaptive immune response.

Supplementary Figures and Tables

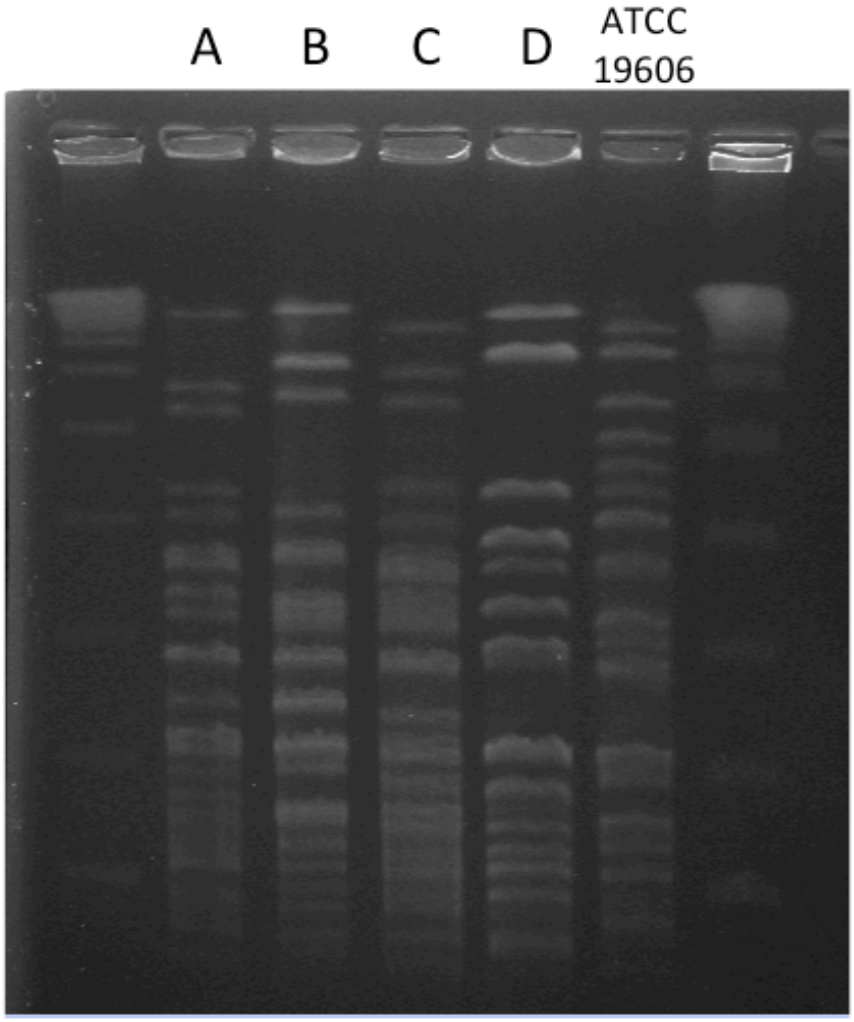

Figure S1 – Pulsed-Field gel electrophoresis comparing major MDR strain types observed during outbreaks at the NIH Clinical Center. The pulsed-field gel patterns are shown for representatives of the major strain types observed during *A. baumannii* outbreaks at the NIH Clinical center(Snitkin et al. 2011; Palmore et al. 2011). Types A, B and C are all members of the European Clone II lineage. Type D is a member of the European Clone I lineage.

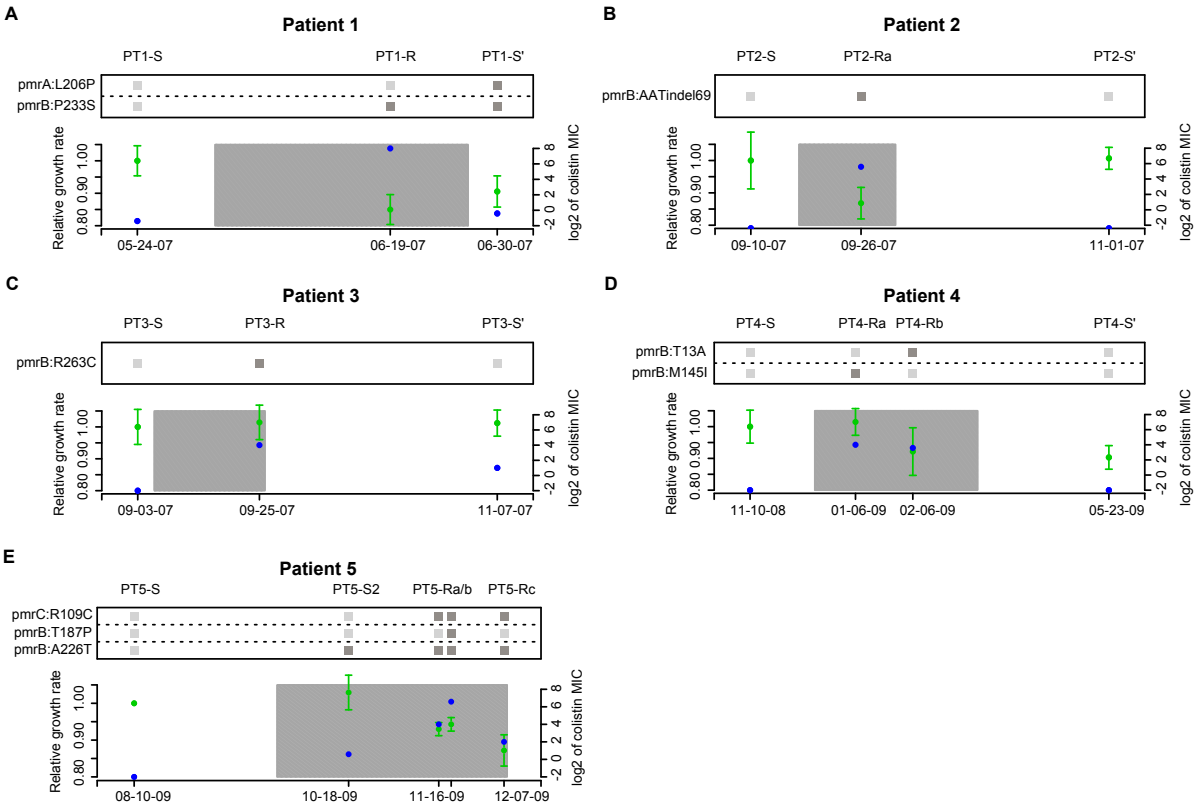

Figure S2 – Relative in vitro growth rates during the evolution of colistin resistance. . The relationship between *pmr* genotype, *in vitro* growth rate and colistin MIC are shown for patients 1 through 5 **(A-E)**. The x-axis of each plot represents time, with the date of each isolate labeled. The left y-axis of each plot represents the growth rate relative to the initial patient isolate, and corresponds to green points. The relative growth rates and error bars are based on the mean and standard error of three replicate experiments. The right y-axis of each plot represents the isolates MIC, and corresponds to blue points. The heatmap above represents the presence/absence (dark gray/light gray) of mutations to the *pmr* observed in each patient's isolates.

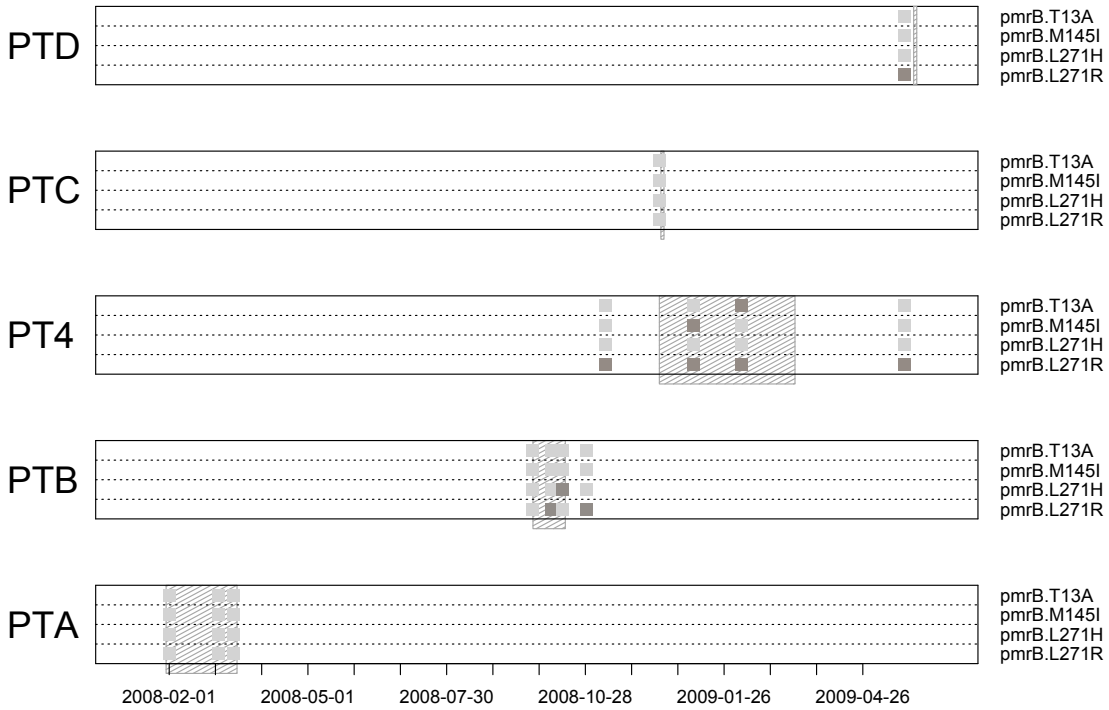

Figure S3 – *pmr* genotype for patients whom might have transmitted/acquired resistant strain to/from patient 4. The *pmr* genotypes for patient 4 (PT4) from the main text, as well as four other patients treated with colistin (PTA – PTD) are shown over time. Patients A-D were selected based on: 1) having a type B strain of *A. baumannii* isolated during 2008 or 2009 and 2) having received colistin treatment. Note that PTA and PTC received only prophylactic colistin treatment for 2 days, because it was determined that their *A. baumannii* isolates were not causing infection. Isolates with the same *pmr* genotype as PT4-S were taken from PTB and PTD, who we hypothesized transmitted to and acquired from PT4, respectively.

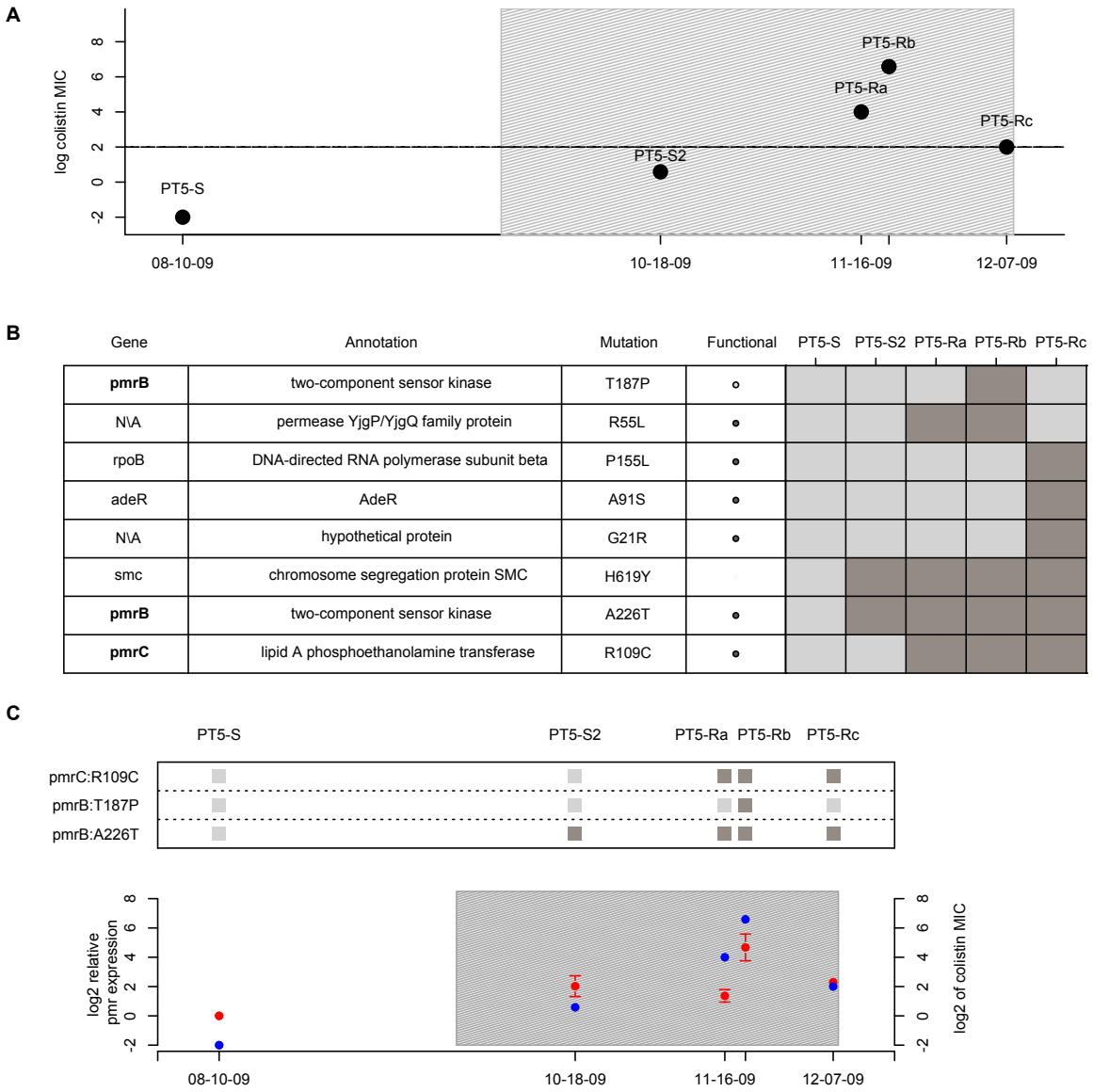

Figure S4 – Resistance, genotype and pmr expression for isolates from patient 5. In addition to the four patients discussed in the main text, there was a fifth patient in which colistin resistance evolved. This patient was not discussed in the main text because they never were taken off colistin, and therefore could not provide insight into the fate of resistance mutations. **(A)** The colistin minimal inhibitory concentration (MIC) of *A. baumannii* isolates from patient 5 is shown The x-axis represents time, with the shaded box indicating the time period during which the

patient received colistin. The y-axis shows the colistin MIC, with the horizontal line drawn at an MIC value of 4, which is the clinical cutoff for colistin resistance. **(B)** Rows represent all nonsynonymous mutations identified across the genomes of the patient isolates. Isolates are shown in temporal order, in the columns of the heatmap. Dark gray/light gray boxes in the heatmap represent the presence/absence of mutations in each isolate. The *pmr* genes are bolded, to emphasize their mutation in the resistant isolates. **(C)** The relationship between *pmr* genotype, *pmr* transcript level and colistin MIC are shown. The x-axis represents time, with the date of each isolate labeled. The left y-axis represents the *pmr* expression relative to the initial patient isolate, and corresponds to red points. The expression values and error bars are based on the mean and standard error of three replicate experiments. The right y-axis represents the isolates MIC, and corresponds to blue points. The heatmap above represents the presence/absence (yellow/gray) of mutations to the *pmr* observed in each isolate.

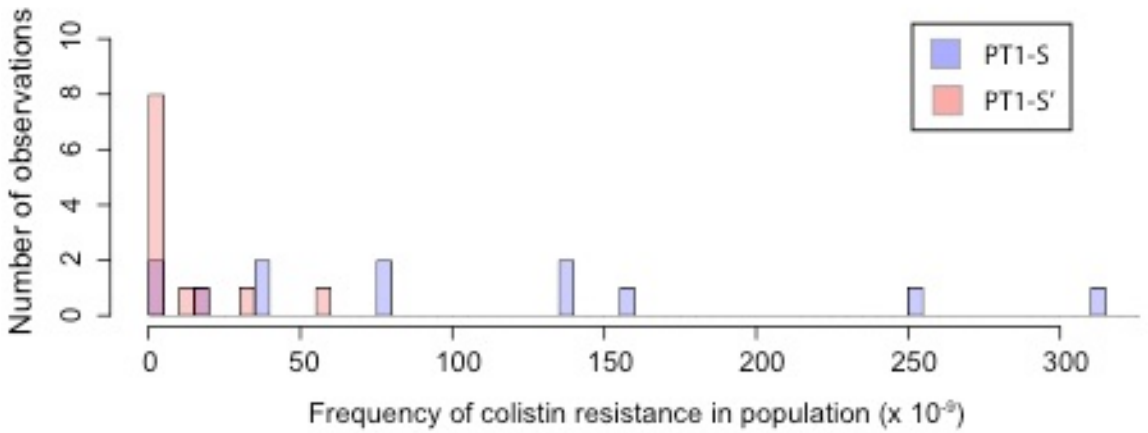

Figure S5 – Frequency of colistin resistant mutants in populations of PT1-S and PT1-S'. Fluctuation tests were performed as discussed in the main text and described in the Methods section. When performing fluctuation tests the number of resistant clones in a population are determined. This was done for colistin susceptible strains taken from patient 1, before (PT1-S) and after (PT1-S') colistin treatment. The frequency of resistant clones in the populations after growth of 14 independent cultures is shown as overlaid histograms for PT1-S (blue) and PT1-S' (red). Magenta represents red overlaid on blue, or in other words PT1-S and PT1-S' both having a given count. The results of these experiments were used to determine the rate of mutations that confer colistin resistance and to show that PT1-S has a significantly increased rate compared with PT1-S' (See main text).

Strain	Patient	Date of isolation	Colistin MIC	Pulsotype	Site
PT1-S	PT1	5/24/07	0.38	A	Sputum
PT1-R	PT1	6/19/07	256	A	Tracheal aspirate
PT1-S'	PT1	6/30/07	0.75	A	Bronchoalveolar lavage
PT2-S	PT2	9/10/07	0.19	B	Groin
PT2-Ra	PT2	9/26/07	48	B	Tracheal aspirate
PT2-Rb	PT2	10/2/07	32	B	Tracheal aspirate
PT2-Rc	PT2	10/10/07	12	B	Tracheal aspirate
PT2-S'	PT2	11/1/07	0.19	B	Sputum
PT3-S	PT3	9/3/07	0.25	B	Tracheal aspirate
PT3-R	PT3	9/25/07	16	B	Tracheal aspirate
PT3-S'	PT3	11/7/07	2	A	Sputum
PT4-S	PT4	11/10/08	0.25	B	Bronchoalveolar lavage
PT4-Ra	PT4	1/6/09	16	B	Sputum
PT4-Rb	PT4	2/6/09	12	B	Sputum
PT4-S'	PT4	5/23/09	0.25	B	Tracheal aspirate
PT5-Sa	PT5	8/10/09	0.25	D	Tracheal aspirate
PT5-Sb	PT5	10/18/09	1.5	D	Bronchoalveolar lavage
PT5-Ra	PT5	11/16/09	16	D	Tracheal aspirate
PT5-Rb	PT5	11/20/09	96	D	Tracheal aspirate
PT5-Rc	PT5	12/7/09	4	D	Tracheal aspirate

Table S1 – Summary of sequenced isolates.

	A	B	C	D
Amikacin	<=16 (S)	>32 (R)	>32 (R)	>32 (R)
Amp/Sulbactam	NA	>16/8 (R)	>16/8 (R)	32 (R)
Aztreonam	>16 (R)	>16 (R)	>16 (R)	16 (I)
Cefepime	16 (I)	>16 (R)	16 (I)	>16 (R)
Ceftazidime	>16 (R)	>16 (R)	>16 (R)	>16 (R)
Ciprofloxacin	>2 (R)	>2 (R)	>2 (R)	>2 (R)
Colistin	0.25 (S)	0.5 (S)	0.125 (S)	0.125 (S)
Gentamicin	>8 (R)	>8 (R)	>8 (R)	>8 (R)
Imipenem	>32 (R)	>8 (R)	<=4 (S)	>8 (R)
Levofloxacin	>4 (R)	>4 (R)	>4 (R)	>4 (R)
Meropenem	>8 (R)	>8 (R)	8 (I)	>8 (R)
Pip/Tazo	>64 (R)	>64 (R)	>64 (R)	>64 (R)
Rifampin	NA	4	4	NA
Ticar/K Clavulanate	64 (I)	>64 (R)	>64 (R)	>64 (R)
Tigecycline	4	2	2	NA
Tobramycin	<=4 (S)	>8 (R)	>8 (R)	<=4 (S)
Trimeth/Sulfa	>2/38 (R)	>2/38 (R)	>2/38 (R)	>2/38 (R)

Table S2 – Antibiotic resistance panel outbreak strains upon first detection at NIH Clinical Center.

Locus Tag	Strain	Mean/median depth	Number of contigs	Contig N50	Number of bases	Number of protein coding genes
ABNIH1	PT1-S	29/23	103	81821	3905549	3884
	PT1-R	31/28	88	88296	3906088	3822
ABNIH5	PT1-S'	16/15	167	49766	3941913	3785
ABNIH2	PT2-S	22/19	125	78659	3952053	3859
	PT2-Ra	24/21	130	70376	3949413	3857
ABNIH13	PT2-Rb	29/28	257	32903	3951678	3929
ABNIH14	PT2-Rc	83/82	220	39582	3961440	3928
ABNIH15	PT2-S'	65/64	225	33386	3904542	3827
ABNIH17	PT3-S	64/63	291	30988	4003054	4004
ABNIH16	PT3-R	34/31	217	37365	4047096	4038
ABNIH18	PT3-S'	43/41	178	51443	3974121	3866
ABNIH24	PT4-S	68/69	360	24460	3842708	3832
ABNIH23	PT4-Ra	61/60	243	32579	3927317	3899
ABNIH20	PT4-Rb	92/93	310	28608	3895296	3884
ABNIH22	PT4-S'	69/69	216	38854	3942007	3916
ABNIH19	PT5-Sa	66/65	153	66616	3982952	3869
ABNIH6	PT5-Sb	14/13	163	50876	3991796	3841
ABNIH7	PT5-Ra	9/10	443	15467	3954057	4023
ABNIH9	PT5-Rb	14/13	214	36816	3969540	3901
ABNIH10	PT5-Rc	8/9	813	7877	3899672	4167

Table S3 – Genome sequencing and assembly statistics for sequenced strains.

Strain	E-test MIC	Broth Microdilution MIC
PT1-S	0.125	1
PT1-R	256	128
PT1-S'	0.125	1
PT2-S	0.125	1
PT2-Ra	256	128
PT2-Rb	32	128
PT2-Rc	8	128
PT2-S'	0.125	1
PT3-S	0.125	1
PT3-R	16	128
PT3-S'	2	1
PT4-S	0.125	64
PT4-Ra	16	128
PT4-Rb	24	128
PT4-S'	0.125	1
PT5-S	0.125	1
PT5-S2	0.125	1
PT5-Ra	48	128
PT5-Rb	256	128
PT5-Rc	4	64

Table S4 – Minimal inhibitory concentrations by E-test and broth microdilution.

E. coli gene (amino acid)	A. baumannii gene (amino acid)	Mutation	Phenotype	Current Strain
envZ(241)	pmrB(226)	envZ(V241G)	Activation	PT5-S2(A226T)
envZ(248)	pmrB(233)	envZ(P248L)	Activation	PT1-R(P233S)
envZ(273)	pmrB(260)	envZ(D273Y)	Activation	PT3-R(R263C)
envZ(283)	pmrB(270)	envZ(Q283P)	Activation	PT4-S(L271R)
ompR(212)	pmrA(206)	ompR(V212A)	No Binding	PT1-S'(L206P)

Table S5 – Mapping of functionally relevant mutations identified in mutatgenesis studies of envZ and ompR to mutations in current study found in pmrB and pmrA, respectively

Amplimer	Left primer	Right primer
1	ACGTGCTTACTTTTATTTATTCTCC	AAGAAGATCTGTTTATCGATATCTG
2	CTATACCTTGAGCGGTTTTATGAGA	CACTCTTGTGCCCATGTAAACTA
3	CCAAACCATCTAAACCGTTATTGAC	GCGGTTTTACAAATCTTAAATTGGA
4	TCTAGTAAACCTTCGCGGTGACTGG	CATACGCAGTAGATGGGAATTCTAT

Table S6 – Primers used to sequence *pmr* locus

Nested Sequencing Primer	
1	ACCAACTGCTCCACACAA
2	AAGATGCTCATCAAGTTCAGCGC
3	CGGTTTAAAGGGTTGATATGCTT

Table S7 – Nested primers used for sequencing of the *pmr* locus

Supplementary References

Antunes, L. C. S., Imperi, F., Towner, K. J. & Visca, P. Genome-assisted identification of putative iron-utilization genes in Acinetobacter baumannii and their distribution among a genotypically diverse collection of clinical isolates. *Res Microbiol* (2010).

Bollenbach T, Quan S, Chait R, Kishony R. 2009. Nonoptimal Microbial Response to Antibiotics Underlies Suppressive Drug Interactions. *Cell* **139**: 707–718.

Fernández-Reyes, M. *et al.* The cost of resistance to colistin in *Acinetobacter baumannii*: a proteomic perspective. *PROTEOMICS* **9**, 1632–1645 (2009).

López-Rojas R, Domínguez-Herrera J, McConnell MJ, Docobo-Peréz F, Smani Y, Fernández-Reyes M, Rivas L, Pachón J. 2011. Impaired Virulence and In Vivo Fitness of Colistin-Resistant Acinetobacter baumannii. *Journal of Infectious Diseases* **203**: 545 –548.

Palmore TN, Michelin AV, Bordner M, Odom RT, Stock F, Sinaii N, Fedorko DP, Murray PR, Henderson DK. 2011. Use of Adherence Monitors as Part of a Team Approach to Control Clonal Spread of Multidrug-Resistant Acinetobacter baumannii in a Research Hospital. *Infect Control Hosp Epidemiol* **32**: 1166–1172.

Rolain J-M, Roch A, Castanier M, Papazian L, Raoult D. 2011. Acinetobacter baumannii Resistant to Colistin With Impaired Virulence: A Case Report From France. *Journal of Infectious Diseases* **204**: 1146 –1147.

Snitkin, E. S. *et al.* Genome-wide recombination drives diversification of epidemic strains of Acinetobact er baumannii. *Proceedings of the National Academy of Sciences* (2011).